Review Article **ISSN: 2347-4882**

WORLD JOURNAL OF PHARMACOLOGICAL RESEARCH AND TECHNOLOGY

PROSPECTS OF ENHANCING MRI IMAGING OF LUNGS THROUGH HYPERPOLARIZED XE-129: A REVIEW

Yash Dhamija[1], Yunes M.M.A. Alsayadi[1]*

[1]University Institute of Pharma Sciences, Chandigarh University, Gharuan, Mohali, Punjab, India

ABSTRACT

Lung tissue has low proton density which makes its MRIs challenging, as well as the presence of artifacts due to cardiovascular pulsation movement and respiration and air–tissue interfaces. To make the lung MRIs feasible, the idea of using of hyperpolarized noble gases comes to the light. They lead a role that enhance nuclear polarization up to five orders of magnitude, and thus make the MRI signal higher. Hellium-3 (He-3) is the one most commonly used due to its favourable safety profile and strong signal, but its use in other applications has affected its availability. Along with Xe-129 lower cost, it has adverse effects that can be easily resolved within short time after administration. A hyperpolarized Xe-129 was approved in December 2022, by the FDA to be used with MRI for the evaluation of lung ventilation. In this review, different aspects related to Xe-129 have been discussed, including the pathophysiology of lungs, pharmacokinetics and pharmacodynamics of Xe-129. Special attention is paid to various reported clinical trials of Xe-129. A comprehensive literature search was conducted in the relevant databases to identify studies published in this field during recent years. Hyperpolarized Xe-129 is almost similar to non-polarized Xe-129 in its chemistry, and xenon is a clear, inert, stable, noble, colourless, monoatomic, gas. Upon inhalation, the hyperpolarized xenon 129 gas is distributed throughout the lungs. MRI, immediately following HP129Xe administration, allows for the visualization of lung structures based on the distribution pattern of the gas. This may aid in the diagnosis of certain lung abnormalities. Hyperpolarization of Xe 129 enhances NMR signals and thus improves imaging and assessment of lung function.

Keywords: COVID-19, MRI, Xe-129, FDA, etc.

Received 1 May 2023, Revised 12 May 2023, Accepted 15 May 2023

INTRODUCTION

Any issue with the lungs that prevents them from functioning properly is referred to as a lung disease [1]. A crucial component of the respiratory system are the lungs. The lungs absorb oxygen from the surrounding air and circulate it through the body's airways and air sacs when someone breathes. After that, the oxygen is taken up by the blood and transported via the blood arteries to the heart [2]. Lung illness can be of three primary types: 1. Airway illness: These disorders have an impact on the tubes (or airways) that transport air to and from the lungs. Diseases including chronic bronchitis, emphysema, and asthma can constrict or clog these airways, giving you the sensation of breathing through a straw [3]. 2. Diseases of the lung tissue make it challenging for the lungs to function normally and transfer oxygen from the airways into the circulation [2] 3. The Bronchial Flow Disorder (BFD): The majority of lung disorders change the blood flow through the bronchi. The bronchial circulation also plays a significant role in airway illnesses because both inhaled and extracted particles first lodge on the bronchial mucosa, which is only supplied by the bronchial circulation. Increases in bronchial circulation are brought on by lung inflammation, which also serves as the only source of oxygen for scar tissue in the lung. The bronchial circulation enlarges in acute illnesses when regional pulmonary perfusion is decreased due to hypoxic vasoconstriction, intravascular thrombosis, emboli, or external compression of the blood vessels by oedema. As soon as 4 to 5 days following the absence of pulmonary flow, the proliferation of new arteries becomes apparent. The bronchial blood flow may expand significantly under chronic circumstances. It typically accounts for less than 1% of cardiac output, but it has the potential to grow to make up more than one third of the circulatory flow and, in cases of congenital abnormalities, even fully replace the circulatory system in the lungs [4]. Lung cancer: The biggest cause of cancer-related death worldwide is lung cancer. This is primarily due to the fact that it is initially silent and frequently detected at an advanced stage. Low-dose computed tomography (LDCT) screening for lung cancer has just been demonstrated to have a mortality benefit, and usage of this procedure is expanding. There are new guidelines to help in the diagnosis and staging of lung cancer once it has been suspected [5]. NSCLC (84% of all lung cancers) and small cell lung cancer (SCLC) (13% of all lung cancers) are the two primary pathologic groups in which the majority of lung cancers fall [6]. Pathological The pathology classification for the diagnosis of NSCLC begins with a tissue section stained with hematoxylin and eosin being examined under a microscope for morphological alterations to determine the presence of an NSCLC and then trying to classify it as any of the various

subtypes like ADC, SqCC, LCLC, or specific subtypes. But occasionally, the histology assessment can be inadequate, especially in little biopsies or tumours with poor distinction, which can make neoplasm classification difficult. In these situations, auxiliary diagnostic methods will aid in classifying the pathology. TTF-1, p40, and mucicarmine are some of the most important auxiliary diagnostic indicators [7]. The diagnosis, staging, and location of lung cancer are all determined by radiographic imaging, which also influences the choice of the forensic tissue collection method. Because it generates 3-dimensional images of tumours and anatomical structures and detects lymphadenopathy, axial CT is the international standard for staging. The 2-dimensional pictures from a chest radiograph, as previously indicated, only offer little information [6].

However, it is still unclear how COVID-19 will affect patient outcomes in the long run. This study aims to investigate if COVID-19 continues to have impacts on client computed tomography of the chest (CT), pulmonary function, respiratory symptoms, weariness, functioning, quality of life, and ability to resume work after a 3-month follow-up. In order to adjust rehabilitation programmes to the needs of COVID-19 patients and to influence future medical planning and resource allocation, the findings of this study will fill a critical information gap regarding the long-term impact of COVID-19 on patient outcomes [8]. It captures a person's physical, mental, emotional, and/or social well-being as a result of the critical illness's cause, underlying co-morbidities, and treatments, and has grown to be a key indicator of recovery and outcome following a life-threatening illness. The Short Form-36 (SF-36) wellness survey is the most widely used and most thoroughly validated tool for measuring HRQL. The SF-36 is a questionnaire that assesses HRQL across eight domains, four of which—physical functioning, role physical, overall wellness, and bodily pain-are combined to yield a score for the physical component, and four of which-vitality, interaction, emotion role, and mental health index-can be combined to yield a score for the mental component summary [9].

Pulmonary Function Test (PFT)

A PFT may consist of a variety of tests, most frequently spirometry with transfer-volume loop, lung volume, and diffuse lung carbon monoxide (DLCO), though each clinician must choose which parts of the test are necessary for their particular patient. However, it is typically advised that patients refrain from using inhaled bronchodilators or smoking tobacco on the day of the test. It should be noted that each laboratory will give the patient specific instructions prior to the test.[10] PEFR and FEF25-75% ought to be recorded for spirometry. Upper airway blockage (typically accompanied by a plateau in expiratory flow), a lacklustre

expiratory effort, or weak respiratory muscles can all lower PEFR. With interstitial lung disease, PEFR may be beyond normal, and the ratio of% predicted PEFR to% predicted FVC is frequently increased. Occlusion is more likely to be confirmed by a low FEF25-75% in relation to FVC than by a normal or raised FEF25-75% compared to FVC. In addition to reporting PIFR, the chart with pre- and post-bronchodilator circles also shows the projected expiratory flow-volume curve [11]. Many healthcare facilities have limited laboratory-based PFT to crucial cases where results will immediately inform treatment decisions in order to prevent unnecessary harm to patients and professionals within areas with a significant incidence of COVID-19. However, because many now use almost exclusively virtual care for outpatient visits, this has a secondary impact of further restricting the information available to doctors who already have to handle patients without physical examinations. Without this knowledge, managerial choices are made only on the basis of past. When it comes to new patients as well as follow-up patients whose medical condition has altered, this may be sufficient for regular monitoring of certain individuals with stable respiratory disorders but is hard for those patients. As COVID-19 numbers plateau and start to decline, PFT labs may gradually open, but infection control regulations will likely continue to limit testing capacity for a very long time. Since current international recommendations do not differentiate between health-care settings when assessing the hazards of aerosol-generating procedures, concerns about infection prevention and testing capacity will also negatively affect conventional alternatives to in-laboratory testing, such as office-based spirometry. Even the use of spirometer filters does not completely remove the need for improved infection control measures [12]. Diffusing capacity tests should be interpreted using reference values that accurately reflect the population being tested, taking into account adjustments for variables such haemoglobin (Hb) and carboxyhemoglobin (COHb). Given that some projected sets utilise a person's weight as a factor and that most predicted sets are outdated, choosing reference values might be challenging. A clinically significant shift must also be taken into account when interpreting DLCO, and current research indicates that under usual laboratory circumstances, this change could be as much as 20–25% [13].

Computed Tomography

High-resolution non-invasive fast throughput small animal imaging is a problem that can be solved with micro-computed tomography (micro-CT), an x-ray modality. Commercial micro-CT systems to be utilised with living animals have been estimated with dealing with capabilities down to 9 m theoretically by computation of focus spot size, detector pitch, and other geometric variables. The detail of the final image will never be lower because obtaining

perfectly centred projection data is inherently sensitive and because there is loss during the reconstruction process. This kind of data gathering necessitates not just very precise matching of the beam or point at which the direction of projection is rotated, but also perfect object stillness during the acquisition process. Studying the mechanism of respiration, which has significant microstructural dysfunction and physically contracts and expands with each breath, makes this point even more crucial. This organ is particularly challenging to analyse in vivo utilising any imaging modality because of its intricate structure and continual macro movement [14]. Using the previously mentioned complimentary open-source application (Airway Inspector, Brigham and Women's Hospital, Boston, MA), the analysis for LV and other CT indices was carried out. LV, LAA%, and MLD were automatically measured by the software. The software carried out the following process, in brief: The LV was determined by adding the voxels in this attenuation range after the software separated the lung parenchyma from the chest wall and the hilum; The volume of LAA in the lung parenchyma was determined, and LAA% was derived by dividing the total LAA volume by LV. MLD was generated by averaging the CT values of the voxels in the lung parenchyma. This procedure was carried out on both the inhalation and expiratory scans of each patient. A sample of the analysis performed by the software is shown in Figure 1. The changes in LV and MLD (DLV and DMLD) among inhalation and expiratory scans, as well as the E/I ratios of LV and MLD, were ultimately calculated [15]. There have been developed specialised micro-computed tomography (micro-CT) scanners that offer rodents with high-resolution, low-noise CT pictures. These scanners are frequently utilised to noninvasively image rat models of human disease and are readily available on the market. Ex vivo micro-CT scans have been utilised to analyse fresh plucked rat lungs as well as fixed rat lungs to evaluate acute lung injury. Ex vivo micro-CT scans from human lung specimens and Siliastic lung casts made from mice and dogs have been used to segmentation algorithms for quantitative measures of lung microscopic structures and airways. In vivo micro-CT investigations have also been carried out to identify lung tumours and track tumour development and therapy in mice. The rapid breathing rates of mice and rats present extra difficulties for in in vivo examination of rodent lung architecture; Consequently, throughout a micro-CT scan, which may consume up to 30 minutes per scan, multiple breathing loops will take place [16]. It was evident from the 3D bronchial tree visualisation of the three mouse strains that a nomenclature was necessary for relevant cross-correlative investigations. Because of this, we created a term particularly for the mouse airway tree, takes into account the existing, approved nomenclatures for airways and creating a hybrid nomenclature that is anatomically meaningful [17]. Since the CACI

involves an alteration in the ratio of the TLV from advice to expiration, which illustrates the degree of breath hold, inhomogeneity in the breath hold degree among individuals could be corrected [18]. For consistent signal-to-noise ratio (SNR) and lung inflation, as well as for getting repeatable quantitative imaging biomarkers, standardised dosing is crucial. A delivery bag containing HP 129Xe, additional stable Xe isotopes, and buffer gas (nitrogen or helium), which are utilised to customise the overall volume for consistent lung inflation, is used to deliver the dose via inhalation. The amount of Xe gas supplied, the abundance of the isotope 129Xe, and the degree of hyperpolarization are the three dosage attributes that define picture SNR (Figure 1). The dosage equivalent volume (DEV) that was administrated by

$$DEV = f129 \times P129 \times VXe$$

where VXe is the entire volume of xenon gas, P129 is the nuclear spin polarisation of 129Xe, and f129 is the isotopic fraction of that element.

Fig. 1. The chest radiograph and the HP Xe-129 MRI

Conceptually, the DEV is analogous to a 100% isotopically enriched, 100% polarised volume of 129Xe [19].Understanding pulmonary ventilation and perfusion while designing radiation therapy for lung cancer can assist spare functional lung tissue and minimise the effects of the dose-limiting effects of pneumonia and pulmonary fibrosis. Despite examines through helium-3 MR imaging (3He-MRI) and PET (positron emission tomography) have also been

reported, SPECT (single photon emission computed tomography) has been used most frequently to investigate such functional lung reduction treatment planning [20].

Today, the majority of lung diseases are clinically diagnosed primarily based on the patient's medical history and the results of pulmonary function tests (PFTs), which provide an overall evaluation of lung function. Computed tomography (CT) imaging of the lung structure is a helpful adjuvant for some lung illnesses. Although a tool to monitor regional exchange of gases within the lung would be extremely helpful for early evaluation, phenol typing, as well as tracking of lung disease, it is not currently available. The exchange of gases from the lungs from the alveolar airway gaps into the blood through the capillary endothelium and respiratory epithelium is the lung's primary physiological function. The resolution limit of the available in vivo examination modalities is much below the size of important structures, which are on the micrometre scale [21]. There are agents that can be used to enhance the visualization of MRIs imaging of the lungs. These agent lead a role that enhance nuclear polarization up to five orders of magnitude, and thus make the MRI signal higher. Hellium-3 (He-3) is the one most commonly used due to its favourable safety profile and strong signal, but its use in other applications has affected its availability. Along with Xe-129 lower cost, it has adverse effects that can be easily resolved within short time after administration. A hyperpolarized Xe-129 was approved in December 2022, by the FDA to be used with MRI for the evaluation of lung ventilation. **Table.1:** explains the agents that can be used for such purposes along the features of each agent.

Tab.1: Comparison between HP Xe 129 and other agents

Gas Agents	**Features**	**References**
HP 3 He	• Nuclear gyromagnetic ratio (MHz/T) is 33.434 • Polarization is 30-40% • Anoxic nature • Density of the gas (g/cm3) is $1.34*10^{-4}$	[22]

HP 129X	• Nuclear gyromagnetic ratio (MHz/T) is 11.777 • Polarization is 8-25% • Anoxic nature • Density of the gas (g/cm3) is $5.75*10^{-3}$	[23]
1 H/O2 Enhanced	• Nuclear gyromagnetic ratio (MHz/T) is 42.576 • Polarization is 1 ppm • Norm/hyperoxic nature • Density of the gas (g/cm3) is $1.43*10^{-3}$	[24]
SF6	• Nuclear gyromagnetic ratio (MHz/T) is 40.052 • Polarization is 1 ppm • Normoxic nature • Density of the gas (g/cm3) is $6.51*10^{-3}$	[25]
C2F6	• Nuclear gyromagnetic ratio (MHz/T) is 40.052 • Polarization is 1 ppm • Normoxic nature • Density of the gas (g/cm3) is $6.16*10^{-3}$	[26]

HPX_MRI

A easily accessible polarizer (Model 9300, Polarean, Durham, NC) was used to polarise 1-L bags of HP-enriched xenon gas (87% 129Xe) to 10-15% for imaging. A total of 13 slices with a maximum width of 15 mm and a field of view of 32 cm were used to acquire time-series HPX images in the coronal plane, and an image matrix with a size of 128 128 was used to build the images. With time-series HPX-MRI as the fig. 1 shows, 8 sets of volume images were acquired in a single breath-hold of 20 seconds using 8-interleave spiral k-space

sampling, which resulted in a time delay of 2.5 seconds for each volume image (i.e., a temporal resolution of 2.5 seconds) and a pixel determination of 2.5 mm (spatial resolution 2-3 mm) . Similar to the concepts of SPECT relative circulation and respiration (i.e., relative SPECT-%perfusion and relative SPECT-%ventilation), the time-series HPX-MRI permitted the computation of the relative percentage respiration (i.e., relative HPX-%ventilation). In addition, the total percentage ventilation (also known as the absolute HPX-%ventilation) was calculated in each lung lobe using a signal threshold method, just like the absolute CT-%emphysema score [27]

Hyperpolarized-Gas Production-

Xenon-129 was polarized using a commercial proto- type system (Xemed LLC, Durham, NH) (18) by means of spin-exchange optical pumping (2,18,19). For each set of experiments, two liters of xenon gas were accumulated in the frozen state. Subsequently, the gas was thawed into four 500-mL Tedlar bags for four breath hold imaging experiments. To maintain at least 21% oxygen entering the lungs, each HXe129 dose was administered together with an oxygen-air mixture as described above [23-27].

Bronchoconstriction and Reversal

The catheter utilised for cleansing the pulmonary circulation was left in place for the animals used in the hp 129Xe MRI tests. To guarantee medication administration to the pulmonary circulation, the cerebral vena cava was strangulated. As described in earlier research (43), the cannula in the caudal vena cava was bound into place and connected to 1.6-mm external diameter perfluoroalkoxy (PFA) tubing for medication administration to the pulmonary circulation. To maintain a steady level of fluid within the ventilated chamber throughout the duration of the imaging studies, extra fluid was evacuated. After imaging, the lungs were inflated 8–10 times with 100% oxygen in an effort to meet tissue metabolic demands. Next, the lungs and transfer channel were purge with N2, followed by the delivery of MCh (with Hartmann's solution) and hp 129Xe. As a result, fewer than 3–4 minutes were spent with the lungs under anoxic conditions [28].

To establish repeatability of hp gas inhalation, initial hp 129Xe magnetic resonance (MR) imaging was regularly carried out at the baseline. Multiple pictures (minimum of two) were captured and visually reviewed to ensure a consistent point of reference for comparing later image information on increasing MCh doses. Furthermore, to make sure there weren't any noticeable changes on the hp 129Xe MRI after the intake of fluids to the lung, 4.5 mL of Hartmann's solution was administered at a rate of 1-2 mL/min prior to bronchoprovocative challenges. Methacholine was administered into the pulmonary circulation as previously

described in order to cause bronchoconstriction. The mean signal strength plus three standard deviations was determined from a 10 * 10 voxel region randomly picked outside the lung region within the imaging limits. Increasing concentrations of 10, 25, 50, 75, 100, 200, and 400 mg of MCh were dissolved in 1 mL of 0.9% saline solution.[29]

Administration:

The first commercialised setup that offered gas polarisations of 30%–40% was used to polarise enriched xenon gas (87% xenon-129). 0.5 L of HXe gas was introduced into a 600 ml Tedlar bag prior to the collecting of MR data. The subjects breathed in the HXe gas via the bag beginning with residual lung volume. As the subjects started to breathe in the air in the room and then maintained their breath at full lung capacity, a helper removed the empty bag from their mouths [30]. Over the past 20 years, it has been demonstrated that hyperpolarized (HP) gas MRI of the lung (3He or 129Xe) is a susceptible imaging tool for examining lung function [31]. The optical diffusion coefficient imaging technique was used to collect the HXe MRI data [31]. The use of xenon-129 (2) as an ingested contrast material for MRI imaging resulted from the discovery of hyperpolarization techniques. Hyperpolarized xenon-129 (HXe129) diffuses from alveolar air gaps into the 5-8 micron-thick alveolar septa during inhalation, following the practical route of gas exchange in the lung [32]. Subjects without access to current (within 6 months) medical pulmonary function tests underwent spirometry. An on-the-go spirometer was used to perform spirometry right before the MRI. The HP 129Xe inhalation dose was $1/6^{th}$ of the expected total lung capacity (TLC), which was determined using the subject's height and the ATS plethysmography-based recommendations for children [33]. In the supervision of a medical expert (an RN or an MD), an experienced member of the study team gave xenon gas. Before inhaling the HP 129Xe gas combination from the functional residual capacity (FRC) via a mouthpiece and bag and an inhale-hold (up to 16 s) while 129Xe ventilation imaging, subjects were instructed to fully inhale to TLC and expel to FRC twice. A digital pulse oximeter that is MR-compatible was used to continuously track the subjects' heart rates and SpO_2 throughout the course of the investigation [34]. One-way ANOVA was used to evaluate the results of the lung function tests for vital capacities, FRC, RV, FVC, FEV1 compared forecasted [%], DLCO Dsb, and 6MWT comparing the three patient groups (i.e., AMN, HS, and COPD). The global null hypothesis, according to which there is no relationship between the mean of the distribution of lung function measurement results and study group, was put to the test using a F test. The Welch 2-sample test, a parametric examination similar to the 2-sample Student's t test but lacking the fundamental assumption of between-group evaluation variability homogeneity,

was used to test hypotheses relating to pairwise between-group contrasts of the averages of lung function measurement distributions [35]. BrukerH Avance III microimaging equipment with a 9.4 T vertical bore is used for pulmonary MRI imaging investigations. All experiments make use of a specially created 25 mm low-pass birdcage volume coil adjusted to the resonant frequency of 129Xe gas in the lung, which is 110.69 MHz. Using 30 diligently pulses of 4.47 msat53 W and the theoretical plans discussed in the Results, spectroscopic data are collected. A customised variable flip angle (VFA) FLASH gradient echo pulse series is used to acquire the images. For non-slice-selective and slice-selective imaging, hard pulses of 134 ms and sinc-shaped pulses of 1000 ms are used at varying power levels. Each phase increment is recorded for 2.61 ms, with following phase increment acquisitions occurring 214.5 ms apart. The overall capture period for a picture with a resolution of 128664 is thus 13.8 s. All parallel photographs are collected in 128664 picture matrices with an overall field perspective (FOV) of 46.9 mm in the superior direction and 30.0 mm in the inferior direction. Slice-selective imaging tests use 4 mm-thick slices, and the central slice's excitation is matched by the slice-selective frequency offset [29]. A large number of patients reported ongoing respiratory symptoms, but all of them also showed some degree of radiological abnormalities. These results were often insignificant, like non-dependent pulmonary fibrosis in 96% of patients. Along with minor abnormalities, more than one-third of patients also had valuable bronchiectasis and/or de novo pulmonary fibrosis [36].

Xenon 129-Mechanism of Action

A prevalent autosomal recessive deadly genetic illness in Caucasians, cystic fibrosis is characterised by improper chloride transport, which leads to substantial, fluid discharges in the airways [37]. The ratings based on the visually perceived proportion of ventilation abnormalities had a reasonable predictive value ($r = 0.42$; $P = 0.04$) when Van Beek et al. evaluated the viability of HP 3He MRI for pediatric patients with cystic fibrosis [38]. After receiving chest physical therapy, MRI is used to evaluate the regional variations in lung respiration, such as percussion and drainage, in children with cystic fibrosis. The researchers discovered that while localised lung ventilation increased but the global lung breathing volumes stayed the same in the majority of patients after therapy, indicating that HP 3He MRI is capable of identifying regional statistical changes in lung breathing following chest physiotherapy [39]. They discovered that although most patients' regional lung ventilation increased after therapy, the global lung airflow volumes stayed unchanged, which suggests that HP 3He MRI is sensitive to identifying regional statistical changes in lung breathing after chest physiotherapy [39]. The mean VDS in patients with cystic fibrosis was higher than that

previously reported for healthy subjects and disparate changes in the circulation and the degree of ventilation flaws were witnessed after a single therapy session, according to Bannier et al., even though pulmonary function tests were regular [40]. A more recent work by Kirby et al. showed the great sensitivity and consistency of HP 3He MRI by showing that it could identify significant changes in ventilation distribution in cystic fibrosis patients that didn't appear in alterations in pulmonary function tests [41]. When inhaled repeatedly for a long duration (min) at concentrations more than 50%, xenon serves as a general anaesthetic. In order to evaluate cerebral blood flow with CT, xenon has been utilised safely for many years [42]; the normal protocol calls for regular inhalation of 33–35% xenon combined with oxygen is for 5 minutes. Latchaw et al. investigated negative reactions to xenon-enhanced CT in a multicenter study encompassing 1830 individuals [43]. In this study, 0.4% of the participants experienced a headache or heavy head. No significant respiratory depression was seen, and blood pressure as well as arterial CO2 pressure remained constant. Four participants (0.2%) experienced partial seizures, however three of them underwent evaluations for known intractable seizure disorders. Three healthy participants were used by Mugler et al. to demonstrate the first MR ventilation pictures and spectroscopy using HP 129Xe [44]. In these early investigations, certain minor side effects were noted, including nausea, lightheadedness, dry mouth, moderate throat irritation, and numbness in the legs. A recent study by Driehuys et al. examined the safety and acceptability of HP 129Xe MRI in both healthy individuals and COPD patients. The majority of patients (91%) had xenon-related symptoms as lightheadedness, the sensation of paresthesia joy, and hypoesthesia, but they all went away on their own in less than 2 minutes [42] According to previously published guidelines, inhaled gas mixtures must contain at least 21% oxygen and no more than 70% HP 129Xe, with a maximum predicted alveolar xenon concentration of 35% [68,80]. Each breath hold is carried out not more than once every five minutes, and breath hold photographs are restricted to 40 seconds for healthy patients and 20 seconds for those with minor to moderate pulmonary illness. Three patients had mild interstitial lung disease (ILD), but Patz et al. assessed 26 subjects and 350 xenon breath hold tests and found no adverse effects or notable fluctuations in blood pressure or saturation levels of oxygen as it is seen in fig. 2 [42]. Using a rubidium spin-exchange system, 3-Helium gas was polarised to 30% (GE Health Care, Princeton, NJ). The dosage for the patients was 5 ml of 3-Helium per kg of body weight, mixed with an equal volume of N2. Active breathing from a Tedlar bag was used to administer the gas combination, and this was followed by continuous, vital-capacity room air inhalation. All studies were conducted under the direction of the Medical

Sciences and Healthcare Products Regulatory Agency [38] because 3-Helium has not yet received approval.

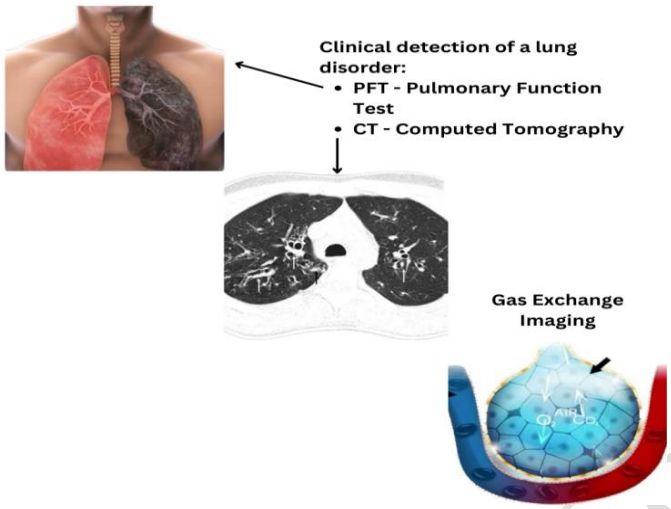

Fig. 2. Mechanism of action of HP Xe 129

Pharmacokinetics

Absorption- Hyperpolarized xenon-129's pharmacokinetic characteristics for absorption are comparable to those of non-polarized xenon. Despite having a low solubility, xenon is more abundant in fatty tissues than in water-soluble tissues and our bodies compartments like plasma.[45] According to a research that modelled the hyperpolarized xenon-129 pharmacokinetics, 80% is the highest concentration that may be breathed. It is possible to find hyperpolarized xenon-129 in the brain and pulmonary tissues after inhalation.[46] Distribution- A rapidly diffusible gas is xenon. After a tiny quantity of xenon is taken up by the pulmonary vessels and distributed to more distant organs, inhaling xenon causes distribution in the well-ventilated parts of the lung. When compared to water-based tissues and our bodies compartments like plasma, fatty tissues have a higher level of xenon solubility.[45] Metabolism- Xenon is not metabolised normally because it is an inert gas. Hepatic or renal function are unaffected by it [47].

Elimination- This research emphasises the potential of hp 129Xe as an ultrasensitive sensor for investigating allosteric sites in proteins. Furthermore, the development of bla as a hyper-CEST the source for biomolecular imaging is supported by the fact that it has a strong track record as a fluorogenic source for in vivo studies. Bla mutagenesis should enable multiplexing or the ability to differentiate over 129Xe-mammalian cell experience signals by increasing Xe binding at the primary site and shifting the hyper-CEST response peak [46].

Pharmacodynamics

The MRI signal produced by hyperpolarized xenon-129 is affected by the amount of gas inhaled, the level of xenon-129 isotopic enhancement, and the level of hyperpolarization. At concentrations greater than 50%, xenon behaves as an anaesthetic when inhaled over an extended period of time. In order to assess cerebral blood flow during computerised tomography (CT) scans, xenon has also been employed. Mathew et al. used the ADC values of the total lung and percent ventilated volume (PVV) to assess radiation-induced damage to the lungs in patients with lung or breast cancer following thoracic radiation therapy as part of treatment evaluation with HP 3He MRI. Their findings indicated that HP 3He MRI was able to identify the physiological compensatory modifications occurring in the contralateral lung as a result of radiation-induced harm in the ipsilateral lung because there were no changes in the ipsilateral lung and only an important rise of PVV in the contralateral lung [74]. According to Allen et al., non-small cell lung cancer patients' HP 3He MRI lung volumes and FEV1 had strong correlations (r2 = 0.89 and 0.83, respectively) prior to and after radiation treatment. This implies that HP 3He MRI may provide crucial functional data as an addition to CT and CT/PET.[42]

Clinical studies

In two prospective, multi-center, randomised, open-label, overlap clinical trials comparing XENOVIEW MRI to xenon Xe 133 imaging in adult patients with pulmonary diseases, Studies 1 (NCT03417687) and 2 (NCT03418090), the safety and effectiveness of XENOVIEW were assessed. 99 mL DE of hyperpolarized xenon Xe 129 at the point of assessment within 5 minutes of administration was the average XENOVIEW dose used in these experiments.

Study 1: XENOVIEW and xenon Xe 133 imaging in patients with respiratory problems such as respiratory mass (44%), COPD (35%), cough (15%), sleep apnea syndrome (12%), and asthma (12%), who were being assessed for potential lung resection surgery. 32 individuals in total, with an average age of 62 years (range: 25 to 77 years), completed both scans. Of them, 78% were White and 69% were male.Six zones made composed of the upper, middle, and lower portions of each lung were used to compute the percentage of the total signal in the lungs for every XENOVIEW and xenon Xe 133 scan.

These figures were used to calculate the afterwards proportion of lung ventilation that was anticipated to last following the deliberate removal of a certain lung region. The primary analysis did not include one among the 32 individuals who underwent both scans because no intended resection region was noted. The remaining 31 patients had a noticed figure of 1.4%

(95% confidence interval: -0.8%, 3.6%) for the mean intra-patient variance in the predicted post-operative percentage of pulmonary ventilation among XENOVIEW and xenon Xe 133 imaging. The percentage of patients who had standardised differences within 10%, 15%, and 20% were 81% (25/31), 94% (29/31), and 94% (29/31) in an exploratory analysis that standardised the inside of-patient variance of the estimated staying lung air circulation between XENOVIEW and xenon Xe 133 visualisation to each patient's xenon Xe 133 results.[45] The most prevalent, fatal hereditary disease affecting Caucasians is cystic fibrosis (CF). The protein known as cystic fibrosis trans membrane conductance regulator (CFTR), needed to control the elements of perspiration, digestive fluids, and mucus, is produced by the gene that causes CF. CFTR gene mutations typically result in aberrant chloride ion transport through the airway epithelium, which results in the production of extremely dense and viscous mucus. The mucus plugs the airways rather than acting as a lubricant, which reduces lung airflow and makes an ideal environment for longterm airway infections. Cysts and scar tissue (fibrosis) development in the lungs are two potential signs of permanent injury. Additionally, the pancreas is obstructed by the thick mucus, which prevents enzymes for digestion from reaching the intestines. Around 70,000 kids and teenagers are thought to have received CF diagnoses globally, with 30,000 cases occurring only in the USA. Sweat tests or genetic testing used to detect this condition are often used in the early stages of infancy.[45-47] **Table 2:** Clinical trials for HP Xe 129 summarizes the details of different clinical trials of HP Xe 129.

Tab. 2: Clinical trials for HP Xe 129

DISEASE AND PHASE	STATUS	INTERVENTION	SPONSOR	ClinicalTrials.gov Identifier	References
E-Cig Use-phase 1 / phase 2	Active and Recruiting	Hyperpolarized Xenon-129 MR Imaging of the Lung:E-cigarette Sub-study	Y. Michael Shim, MD, University of Virginia	NCT04662658	[48]
Chronic Obstructive Pulmonary Disease phase 1 / phase 2	Experimental and Recruiting	COPD patients with standard vs study diagnostic methods (imaging procedures)	Y. Michael Shim, MD, University of Virginia	NCT03331302	[49]
Anoro Ellipta – phase 2	Active and Recruiting	a New Multi-dimensional Biomarker to Determine Pulmonary Physiologic Responses to COPD Therapeutics	Y. Michael Shim, MD, University of Virginia	NCT03002389	[50]
Cannabis Smoking	Not yet recruiting	Diagnostic Test: Computed Tomography (CT)	Grace E Parraga, PhDRobarts Research Institute, The University of Western Ontario	NCT03909477	[51]
Carcinoma, Non-Small-	Active and Recruiting	Combination Product: Hyperpolarized xenon M	Xemed LLC	NCT05302817	[52]

Cell Lung – phase 1		RI			
Bronchopulmonary Dysplasia	Active and Recruiting	Hyperpolarized 129Xe MRI	Parameswaran Nair, Professor of Medicine, McMaster University	NCT03455686	[53]
Asthma –phase 3	completed	Dupilumab / Dupixent Biological: Placebo	McMaster University	NCT03884842	[54]
Fibrosis-phase 3	completed	hyperpolarized Xenon gas	Jason Woods, PhD, Director, Center for Pulmonary Medicine Imaging Research, Principal Investigator, Children's Hospital Medical	NCT03593434	[56]

			Center, Cincinnati		
Chronic Obstructive Pulmonary Disease phase 1 / phase 2	Terminated	Hyperpolarized 129Xe gas	Samuel Patz, Scientific Director, Center for Pulmonary Functional Imaging, Brigham	NCT01697332	[57]
Respiratory DiseaseHealthy	Active and Recruiting	1H and Xe-129 MRI	Jonathan Rayment, Clinical Assistant Professor, University of British Columbia	NCT05102825	[58]
Cystic Fibrosis-phase 4	Active, not recruiting	Hyperpolarized Xenon	Jason Woods, PhD, Children's Hospital Medical Center, Cincinnati	NCT02848560	[59]
Chronic	Recruiting	Azithromycin	Genentech, Inc.	NCT0435366	[60]

Obstructive Pulmonary Disease-phase2				1	

Primary Ciliary Dyskinesia	Recruiting	lung disease include pulmonary function tests (PFT), chest x rays and chest CTs	Felix Ratjen, Principle investigator, The Hospital for Sick Children	NCT04858191	[61]
Diagnosis of Pulmonary Vascular Disease-phase 2	Completed	XeMRI scans will provide 3D images of ventilation and gas exchange. Subjects will inhale HP **129**Xe from the dose delivery bags.	Bastiaan Driehuys, Professor, Duke University Medical Center, Duke University	NCT03078192	[62]

Pulmonary Surgical Procedures-phase 3	Completed	**129Xenon** MRI	Polarean, Inc.	NCT03418090	**[63]**
Asthma – phase 3	Withdrawn	High Dose Dual Therapy (ICS/LABA)	Dr. Grace Parraga, Professor, Western University, Canada	NCT04206761	**[64]**
Pulmonary Surgical Procedures-phase 3	Completed	**129**Xe MRI	Polarean, Inc.	NCT03417687	[65]
Cystic Fibrosis-phase 4	Active, not recruiting	Hyperpolarized **Xenon 129**	Children's Hospital Medical Center, Cincinnati	NCT04467957	[66]

Obstructive Sleep Apnea-phase 4	Recruiting	**129**-Xe	Children's Hospital Medical Center, Cincinnati	NCT04991389	[67]
Lung Disease-phase not applicable	Unknown	MRI at baseline and over time	Dr. Grace Parraga, PhD, Scientist. Robarts Research Institute, Western University, Canada	NCT02723474	[68]
Alpha 1-Antitrypsin Deficiency-phase not applicable	Recruiting	Hyperpolarized **129**Xe MRI	Parameswaran Nair, Professor of Medicine, McMaster University	NCT03455686	[69]

Bronchopulmonary Dysplasia phase – not applicable	Unknown	Hyperpolarized **Xenon-129**	Dr. Grace Parraga, PhD, Scientist, Robarts Research Institute, Western University, Canada	NCT02723513	[70]

Adverse and Side Effects

Xenon xe 129 hyperpolarized may have various undesirable effects in addition to its essential functions. There could be some adverse effects, but they often don't require medical treatment. During treatment, these side effects might go away as your body gets used to the medication.[58]such as a headache, throat and mouth soreness, and weakness.[59]

If any of the adverse effects—whose frequency is unknown and occur, such as disorientation, dizziness, problems with a fast heartbeat, and abnormal breathing—check with your healthcare provider or nurse right away.[58]

If you experience any of the following serious side effects, such as sudden loss of vision, blurred vision, tunnel vision, severe eye pain or swelling, impaired speech, trouble getting around, loss of coordination, feeling unstable, very stiff muscles, a high fever, excessive sweating, or tremors, seek medical attention right away or dial 911.[60]

CONCLUSIONS

In order to more fully understand lung diseases and solve mysteries in respiratory medicine, 129Xe MRI offers rapid, sensitive, non-invasive, and simultaneous measurements of pulmonary ventilation, lung tissue microstructure, as well as diffusion within the alveolus and into the alveolar tissue and red blood cells. The hyperpolarized xenon 129 gas is dispersed throughout the lungs upon breathing. Following the administration of HP129Xe, MRI enables the visualisation of lung structures based on the gas distribution pattern. This might help in making a diagnosis of some lung problems. Hyperpolarization of Xe 129 improves lung function imaging and assessment by enhancing NMR signals.

ACKNOWLEDGMENT

The authors are heartily thankful to the management of Chandigarh University for constant encouragement, support and motivation.

REFERENCES

1. U. S. News, “Lung disease Managing COPD Quiz”.
2. C. Airway, “Lung diseases : What to know,” pp. 1–11, 2021.
3. U. States, “Lung Diseases Types of Lung Disease,” pp. 1–4.
4. J. Butler, “The Bronchial Circulation,” *Physiology*, vol. 6, no. 1, pp. 21–25, 1991, doi: 10.1152/physiologyonline.1991.6.1.21.
5. F. Nasim, B. F. Sabath, and G. A. Eapen, “Lung Cancer,” *Med. Clin. North Am.*, vol. 103, no. 3, pp. 463–473, 2019, doi: 10.1016/j.mcna.2018.12.006.
6. H. Hoy, T. Lynch, and M. Beck, “Surgical Treatment of Lung Cancer,” *Crit. Care Nurs. Clin. North Am.*, vol. 31, no. 3, pp. 303–313, 2019, doi: 10.1016/j.cnc.2019.05.002.
7. J. Rodriguez-Canales, E. Parra-Cuentas, and I. I. Wistuba, “Diagnosis and molecular classification of lung cancer,” *Cancer Treat. Res.*, vol. 170, pp. 25–46, 2016, doi: 10.1007/978-3-319-40389-2_2.
8. D. C. Sanchez-ramirez, K. Normand, Y. Zhaoyun, and R. Torres-castro, “Long-Term Impact of COVID-19 : A Systematic Review of the Literature and Meta- Analysis,” vol. 9, no. July, pp. 1–18, 2021, doi: 10.3390/biomedicines9080900.
9. M. E. Wilcox and M. S. Herridge, “Lung function and quality of life in survivors of the acute respiratory distress syndrome (ARDS),” *Press. Medicale*, vol. 40, no. 12 PART 2, pp. e595–e603, 2011, doi: 10.1016/j.lpm.2011.04.024.
10. T. M. Dempsey and P. D. Scanlon, “Pulmonary Function Tests for the Generalist: A Brief Review,” *Mayo Clin. Proc.*, vol. 93, no. 6, pp. 763–771, 2018, doi:

10.1016/j.mayocp.2018.04.009.

11. U. Industries and S. P. Sintering, "工作计划（徐军）- Page 1 of 3," vol. 11, no. January, pp. 5–7, 2008, [Online]. Available: https://www.nhs.uk/translationspanish/Documents/anorexia_nervosa_spanish_FINAL.pdf
12. A. Kouri *et al.*, "Addressing Reduced Laboratory-Based Pulmonary Function Testing During a Pandemic," *Chest*, vol. 158, no. 6, pp. 2502–2510, 2020, doi: 10.1016/j.chest.2020.06.065.
13. G. L. Ruppel and P. L. Enright, "Pulmonary function testing," *Respir. Care*, vol. 57, no. 1, pp. 165–175, 2012, doi: 10.4187/respcare.01640.
14. E. Namati *et al.*, "In vivo micro-CT lung imaging via a computer-controlled intermittent iso-pressure breath hold (IIBH) technique," *Phys. Med. Biol.*, vol. 51, no. 23, pp. 6061–6075, 2006, doi: 10.1088/0031-9155/51/23/008.
15. T. Yamashiro *et al.*, "Collapsibility of Lung Volume by Paired Inspiratory and Expiratory CT Scans. Correlations with Lung Function and Mean Lung Density," *Acad. Radiol.*, vol. 17, no. 4, pp. 489–495, 2010, doi: 10.1016/j.acra.2009.11.004.
16. N. L. Ford, E. L. Martin, J. F. Lewis, R. A. W. Veldhuizen, M. Drangova, and D. W. Holdsworth, "In vivo characterization of lung morphology and function in anesthetized free-breathing mice using micro-computed tomography," *J. Appl. Physiol.*, vol. 102, no. 5, pp. 2046–2055, 2007, doi: 10.1152/japplphysiol.00629.2006.
17. J. Thiesse *et al.*, "Lung structure phenotype variation in inbred mouse strains revealed through in vivo micro-CT imaging," *J. Appl. Physiol.*, vol. 109, no. 6, pp. 1960–1968, 2010, doi: 10.1152/japplphysiol.01322.2009.
18. K. Suzuki, K. Seyama, H. Ebana, T. Kumasaka, and R. Kuwatsuru, "Quantitative analysis of cystic lung diseases by use of paired inspiratory and expiratory ct: Estimation of the extent of cyst-airway communication and evaluation of diagnostic utility," *Radiol. Cardiothorac. Imaging*, vol. 2, no. 2, pp. 1–9, 2020, doi: 10.1148/ryct.2020190097.
19. P. J. Niedbalski *et al.*, "Protocols for multi-site trials using hyperpolarized 129Xe MRI for imaging of ventilation, alveolar-airspace size, and gas exchange: A position paper from the 129Xe MRI clinical trials consortium," *Magn. Reson. Med.*, vol. 86, no. 6, pp. 2966–2986, 2021, doi: 10.1002/mrm.28985.
20. B. A. Tahir *et al.*, "Spatial Comparison of CT-Based Surrogates of Lung Ventilation With Hyperpolarized Helium-3 and Xenon-129 Gas MRI in Patients Undergoing

Radiation Therapy," *Int. J. Radiat. Oncol. Biol. Phys.*, vol. 102, no. 4, pp. 1276–1286, 2018, doi: 10.1016/j.ijrobp.2018.04.077.

21. I. Dregely *et al.*, "Hyperpolarized Xenon-129 gas-exchange imaging of lung microstructure: First case studies in subjects with obstructive lung disease," *J. Magn. Reson. Imaging*, vol. 33, no. 5, pp. 1052–1062, 2011, doi: 10.1002/jmri.22533.
22. O. Doganay *et al.*, "Fast dynamic ventilation MRI of hyperpolarized 129Xe using spiral imaging," *Magn. Reson. Med.*, vol. 79, no. 5, pp. 2597–2606, 2018, doi: 10.1002/mrm.26912.
23. A. Cho, "Helium-3 shortage could put freeze on low-temperature research," *Science (80-.).*, vol. 326, no. 5954, pp. 778–779, 2009, doi: 10.1126/science.326_778.
24. S. Fain, M. L. Schiebler, D. G. McCormack, and G. Parraga, "Imaging of lung function using hyperpolarized helium-3 magnetic resonance imaging: Review of current and emerging translational methods and applications," *J. Magn. Reson. Imaging*, vol. 32, no. 6, pp. 1398–1408, 2010, doi: 10.1002/jmri.22375.
25. G. Leung, R. H. Ireland, J. Parra-robles, H. Marshall, and J. M. Wild, "Lung ventilation volumetry with same-breath acquisition of hyperpolarized gas and proton MRI," no. January, pp. 1461–1467, 2014, doi: 10.1002/nbm.3187.
26. Y. V Chang and M. S. Conradi, "Relaxation and diffusion of perfluorocarbon gas mixtures with oxygen for lung MRI," vol. 181, pp. 191–198, 2006, doi: 10.1016/j.jmr.2006.04.003.
27. S. Laukemper-ostendorf *et al.*, "F-MRI of Perflubron for Measurement of Oxygen Partial Pressure in Porcine Lungs During Partial Liquid Ventilation," vol. 89, no. September 2000, pp. 82–89, 2002, doi: 10.1002/mrm.10008.
28. D. M. L. Lilburn *et al.*, "Investigating lung responses with functional hyperpolarized xenon-129 MRI in an ex vivo rat model of asthma," *Magn. Reson. Med.*, vol. 76, no. 4, pp. 1224–1235, 2016, doi: 10.1002/mrm.26003.
29. D. M. L. Lilburn *et al.*, "Validating Excised Rodent Lungs for Functional Hyperpolarized Xenon-129 MRI," *PLoS One*, vol. 8, no. 8, 2013, doi: 10.1371/journal.pone.0073468.
30. K. Ruppert, K. Qing, J. T. Patrie, T. A. Altes, and J. P. Mugler, "Using Hyperpolarized Xenon-129 MRI to Quantify Early-Stage Lung Disease in Smokers," *Acad. Radiol.*, vol. 26, no. 3, pp. 355–366, 2019, doi: 10.1016/j.acra.2018.11.005.
31. L. Ebner, "The Role of Hyperpolarized 129 Xenon in MR Imaging of Pulmonary Function Abstract : In the last two decades , functional imaging of the lungs using

hyperpolarized noble gases has entered the clinical stage . Both helium (3 He) and xenon (129 Xe) gas h," pp. 0–36, 2016.

32. E. R. Weibel, "What makes a good lung? The morphometric basis of lung function," *Swiss Med. Wkly.*, vol. 139, no. 27–28, pp. 375–386, 2009.
33. J. A. Neder, S. Andreoni, A. Castelo-Filho, and L. E. Nery, "Reference values for lung function tests. I. Static volumes," *Brazilian J. Med. Biol. Res.*, vol. 32, no. 6, pp. 703–717, 1999, doi: 10.1590/S0100-879X1999000600006.
34. R. P. Thomen, L. L. Walkup, D. J. Roach, Z. I. Cleveland, J. P. Clancy, and J. C. Woods, "Hyperpolarized 129Xe for investigation of mild cystic fibrosis lung disease in pediatric patients," *J. Cyst. Fibros.*, vol. 16, no. 2, pp. 275–282, 2017, doi: 10.1016/j.jcf.2016.07.008.
35. G. D. Ruxton, "The unequal variance t-test is an underused alternative to Student's t-test and the Mann-Whitney U test," *Behav. Ecol.*, vol. 17, no. 4, pp. 688–690, 2006, doi: 10.1093/beheco/ark016.
36. M. E. Wilcox *et al.*, "Radiologic outcomes at 5 years after severe ARDS," *Chest*, vol. 143, no. 4, pp. 920–926, 2013, doi: 10.1378/chest.12-0685.
37. M. J. Welsh and C. M. Liedtke, "Chloride and potassium channels in cystic fibrosis airway epithelia," *Nature*, vol. 322, no. 6078, pp. 467–470, 1986, doi: 10.1038/322467a0.
38. E. J. R. van Beek *et al.*, "Assessment of lung disease in children with cystic fibrosis using hyperpolarized 3-Helium MRI: Comparison with Shwachman score, Chrispin-Norman score and spirometry," *Eur. Radiol.*, vol. 17, no. 4, pp. 1018–1024, 2007, doi: 10.1007/s00330-006-0392-1.
39. N. Woodhouse, J. M. Wild, E. J. R. Van Beek, N. Hoggard, N. Barker, and C. J. Taylor, "Assessment of hyperpolarized 3He lung MRI for regional evaluation of interventional therapy: A pilot study in pediatric cystic fibrosis," *J. Magn. Reson. Imaging*, vol. 30, no. 5, pp. 981–988, 2009, doi: 10.1002/jmri.21949
40. E. Bannier *et al.*, "Hyperpolarized 3he MR for sensitive imaging of ventilation function and treatment efficiency in young cystic fibrosis patients with normal lung function," *Radiology*, vol. 255, no. 1, pp. 225–232, 2010, doi: 10.1148/radiol.09090039.
41. M. Kirby *et al.*, "Quantitative Evaluation of Hyperpolarized Helium-3 Magnetic Resonance Imaging of Lung Function Variability in Cystic Fibrosis," *Acad. Radiol.*, vol. 18, no. 8, pp. 1006–1013, 2011, doi: 10.1016/j.acra.2011.03.005.
42. Z. Liu, T. Araki, Y. Okajima, M. Albert, and H. Hatabu, "Pulmonary hyperpolarized

noble gas MRI: Recent advances and perspectives in clinical application," *Eur. J. Radiol.*, vol. 83, no. 7, pp. 1282–1291, 2014, doi: 10.1016/j.ejrad.2014.04.014.

43. R. E. Latchaw, H. Yonas, S. L. Pentheny, and D. Gur, "Adverse reactions to xenon-enhanced CT cerebral blood flow determination," *Radiology*, vol. 163, no. 1, pp. 251–254, 1987, doi: 10.1148/radiology.163.1.3823444.
44. J. P. Mugler *et al.*, "MR imaging and spectroscopy using hyperpolarized 129Xe gas: Preliminary human results," *Magn. Reson. Med.*, vol. 37, no. 6, pp. 809–815, 1997, doi: 10.1002/mrm.1910370602.
45. H. Of *et al.*, "Indications And Usage Xenoview , prepared from the Xenon Xe 129 Gas Blend , is indicated for use with magnetic resonance imaging (MRI) for evaluation of lung ventilation in adults and pediatric patients aged 12 years and older . Limitations of Use XENOV," pp. 1–8, 2022.
46. Y. Wang and I. J. Dmochowski, "An Expanded Palette of Xenon-129 NMR Biosensors," *Acc. Chem. Res.*, vol. 49, no. 10, pp. 2179–2187, 2016, doi: 10.1021/acs.accounts.6b00309.
47. M. Maze, "Action neuroprotectrice préclinique du xénon et implications possibles pour la thérapeutique humaine: un compte rendu narratif," *Can. J. Anesth.*, vol. 63, no. 2, pp. 212–226, 2016, doi: 10.1007/s12630-015-0507-8.
48. Tugasmereka, "LINK 2.pdf." 2017. [Online]. Available: https://tugasmereka.blogspot.com/2017/08/makalah-aksiologi.html
49. A. Ilmu, "Link 1.pdf." 2015. [Online]. Available: http://blognyasharing.blogspot.com/2015/06/makalah-filsafat-ilmu-aksiologi-filsafat.htm
50. H. Ahmad, "Link 3.pdf." 2013. [Online]. Available: https://hidayatullahahmad.wordpress.com/2013/03/17/makalah-filsafat-ilmu-aksiologi/
51. P. Ibeng, "Link 4.pdf." 2020. [Online]. Available: https://pendidikan.co.id/pengertian-aksiologi-aspek-menurut-para-ahli/
52. S. R. Dates, "Study Details Tab Study Overview," pp. 1–8, 2022.
53. R. Clinicaltrials, "Healthy Volunteers and Patients With Lung Disease Study Details Tab Study Overview," pp. 1–11, 202

54. 2.
55. C. Clinicaltrials, “Study Tab Study Overview,” pp. 1–8, 2013.
56. S. R. Dates and R. R. Dates, “Study Details Tab Study Overview,” pp. 1–7, 2018.
57. S. R. Dates, “Monitoring Response to Orkambi in Cystic Fibrosis Lung Disease by Inhaled Xenon MRI Study Details Tab Study Overview,” pp. 1–10, 2022.
58. NCT04353661, “A Study Of ^{129}XE MRI To Assess Disease Progression In Patients With COPD Treated With Or Without Azithromycin And Standard-of-Care Medications,” *https://clinicaltrials.gov/show/NCT04353661*, pp. 1–11, 2023, [Online]. Available: https://www.cochranelibrary.com/central/doi/10.1002/central/CN-02103286/full
59. S. Effects and H. Info, “Xenon Xe 129 Hyperpolarized (Inhalation Route) Your gift holds great power – donate today !,” 2023.
60. F. H. Professionals, “Xenon xe 129 hyperpolarized Side Effects,” pp. 22–23, 2022.
61. P. John, “XENOVIEW SIDE EFFECTS,” pp. 1–26, 2023.
62. P. Study and N. Study, “Trial record 76 of 78 for : xenon 129 Utilizing Hyperpolarized 129Xe Magnetic Resonance Imaging in Children With Primary Ciliary Dyskinesia (PCD MRI),” pp. 2–8, 2021.
63. P. Study and N. Study, “Trial record 76 of 78 for : xenon 129 Utilizing Hyperpolarized 129Xe Magnetic Resonance Imaging in Children With Primary Ciliary Dyskinesia (PCD MRI),” pp. 2–8, 2021.
64. P. Study and N. Study, “Trial record 54 of 78 for : xenon 129 Non-Invasive Diagnosis of Pulmonary Vascular Disease Using Inhaled 129Xe Magnetic Resonance Imaging (XenonMRI),” pp. 1–7, 2022.
65. S. Description, “Trial record 3 of 5 for : xenon 129 | Phase 3 Hyperpolarized Xenon MRI for Assessment of Pulmonary Function in Lung Transplant,” pp. 1–6, 2020.
66. P. Study, “Trial record 5 of 5 for : xenon 129 | Phase 3 Investigating the Effects of QVM149 on MRI Ventilation Defects (XPERTT),” pp. 1–12, 2021.
67. S. Description, “Trial record 2 of 5 for : xenon 129 | Phase 3 Hyperpolarized Xenon MRI for Assessment of Pulmonary Function in Lung

Resection," pp. 1–7, 2022.

68. S. Description, "Trial record 1 of 2 for : xenon 129 | Phase 4 Non-contrast Lung Perfusion Mapping Applied for New Insights in Cystic Fibrosis," pp. 1–8, 2022.
69. P. Study, "Trial record 2 of 2 for : xenon 129 | Phase 4 Improving Outcomes in Pediatric Obstructive Sleep Apnea With Computational Fluid Dynamics (OSA-MRI)," pp. 1–7, 2023.
70. P. Study and N. Study, "Trial record 8 of 9 for : xenon 129 | Phase Not Applicable A Single-Centre Pilot Study Exploring the Utility of Magnetic Resonance Imaging in Patients With Chronic Lung Disease," pp. 1–6, 2019.

***Correspondence Author:** Yunes M.M.A. Alsayadi, University Institute of Pharma Sciences, Chandigarh University, Gharuan, Mohali, Punjab, India